

PROCEEDINGS B

royalsocietypublishing.org/journal/rspb

Research



Article submitted to journal

Subject Category:

Evolution

Subject Areas:

health and disease and epidemiology, biomathematics

Keywords:

cancer, evolutionary dynamics, tumour cell heterogeneity, phenotypic plasticity, mathematical model

Author for correspondence:

Carmen Ortega-Sabater

e-mail:

carmen.ortegasabater@uclm.es

Date of the version:

8th June 2021

Stochastic fluctuations drive non-genetic evolution of proliferation in clonal cancer cell populations

Carmen Ortega-Sabater, Gabriel F. Calvo, and Víctor M.

Pérez-García

Mathematical Oncology Laboratory (MOLAB), Universidad de Castilla-La Mancha, Ciudad Real, 13071, Spain

Evolutionary dynamics allows to understand many changes happening in a broad variety of biological systems, ranging from individuals to complete ecosystems. It is also behind a number of remarkable organizational changes that happen during the natural history of cancers. These reflect tumour heterogeneity, which is present at all cellular levels, including the genome, proteome and phenome, shaping its development and interrelation with its environment. An intriguing observation in different cohorts of oncological patients is that tumours exhibit an increased proliferation as the disease progresses, while the timescales involved are apparently too short for the fixation of sufficient driver mutations to promote an explosive growth. In this paper we discuss how phenotypic plasticity, emerging from a single genotype, may play a key role and provide a ground for a continuous acceleration of the proliferation rate of clonal populations with time. Here we address this question by means of stochastic and deterministic mathematical models that capture proliferation trait heterogeneity in clonal populations and elucidate the contribution of phenotypic transitions on tumour growth dynamics.

2 1 Introduction

3 Evolution is one of the central unifying concepts of biology and a driving force behind life,
4 being a cornerstone of complex systems organization [1]. It is ubiquitous through the natural
5 world from molecules to cells, organisms and populations and in fields as diverse as zoology,
6 botany, microbiology and oncology. Evolutionary changes in the context of asexual reproduction
7 are mainly driven by heritable somatic mutations and epigenetic changes, genetic drift and
8 natural selection. Evolution theory has been classically grounded in genetics and Darwinian
9 selection processes. In the light of evolution, tumour progression has often been explained
10 by looking at the somatic changes of cancer cells [2,3]. However, from this viewpoint, one
11 might incur in some reductionist assumptions that are sometimes in conflict with what is
12 observed during the real course of the disease, including treatment failure and relapse [4].
13 There is a growing interest in studying the evolutionary rules of cancer, and a number of
14 important questions remain open. Increased attention has recently been given to intratumour
15 heterogeneity as its potential role in therapeutic outcome and emergence of drug resistance [5–
16 8]. Intratumour heterogeneity occurs at various levels, including the genome, transcriptome,
17 proteome and phenome [9]. Research has mainly focused on mapping cancer genome instability
18 and driver event mutations conferring a selective advantage to the affected cell clone. Non-genetic
19 instabilities are also relevant since it is known that a single stable genotype may lead to a broad
20 landscape of stable phenotypes [10,11]. Initial states of cancer development imply colonization of
21 novel environments and subsequent stressful conditions [12], which may actually increase traits
22 heritability (understanding heritability as the relation between genetic variance for the trait and
23 the phenotypic variance for the same trait). Phenotypic variance is the result of a compendium
24 of variances: the variance attributed to differences among genotypes, the variance associated
25 exclusively with changes in the environment and the ‘interaction variance’ which represents that
26 some genotypes might respond to the environment in a different way than others [13]. Distinct
27 phenotypic states frequently involve differences in functional cell properties and the proportion
28 of these phenotypes has been related to cancer grade [14,15]. This resembles what occurs in
29 other biological contexts, where a broader population composition, which comprises a higher
30 phenotypic diversity, increases the odds for an adaptive response to external perturbations [16].

31 Recent observations in both *in vivo* murine models and cohorts of cancer patients of different
32 histologies have found a superlinear scaling law relating proliferation and tumour size [17].
33 Also a longitudinal dynamics was observed implying a continuous acceleration of proliferation
34 rates during tumours natural history, which is a dynamical counterpart of the scaling law. This
35 fact was attributed initially to the tumour’s genetic evolutionary dynamics and supported with
36 different mathematical modelling frameworks. However, a closer look at this interpretation raises
37 a number of questions. The results presented in [17] included two studies in animal models
38 that displayed accelerated tumour growth dynamics in the course of one month. Longitudinal
39 volumetric data obtained from images of cancer patients with untreated brain metastasis also
40 showed similar growth patterns. Genetic changes seem to be necessary [18] but not sufficient to
41 generate such an accelerated tumour growth since they require either an extremely high mutation
42 rate, which would be restricted by cell viability, or a long time scale [19] that was not the case in
43 the former results. For these reasons, neither the human data spanning typically few months, nor
44 the animal models data, could be exclusively associated with tumour genetic changes because
45 of the short time scales involved. This raises the question that we wish to explore in this paper:
46 Could there be additional non-genetic evolutionary forces playing a role in accelerating tumour
47 growth as observed in Ref. [17]?

48 The recognition of the role of phenotypic aspects in cancer evolutionary dynamics has elicited
49 a progressive change in perspective from seeing cancer as a ‘genetic disease’ to a broader,
50 ‘developmental’ perspective. Some analogies with embryonic development have been made,
51 rapidly dividing tissues may have evolved increased cancer suppression [41] and phenotypic
52 plasticity in cancer has been biologically addressed in the literature of cancer stem cells [20]. Also

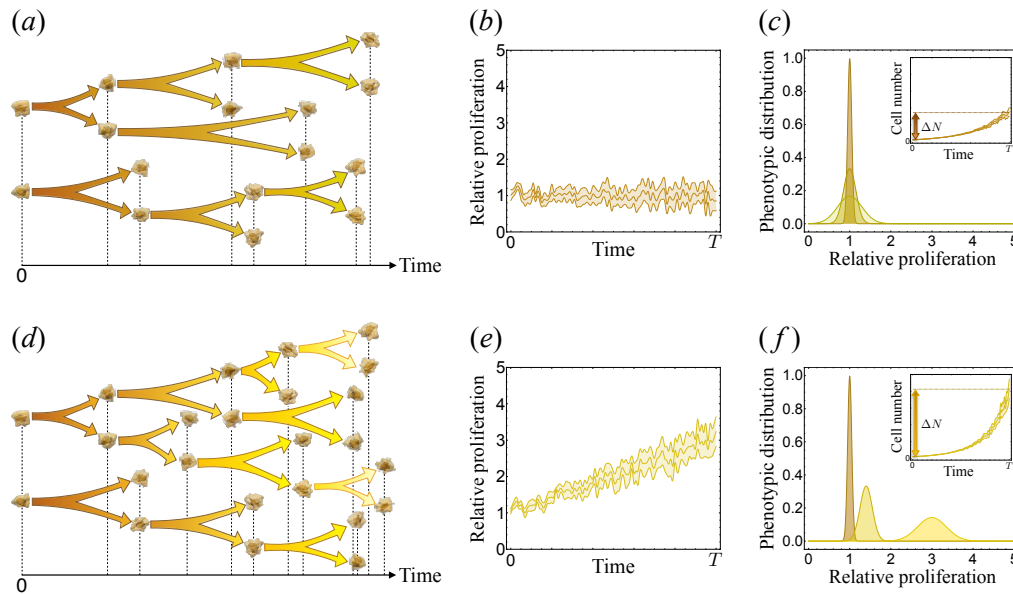


Figure 1. Stochastic fluctuations of cancer cell proliferation in two distinct scenarios: quasi-constant mean proliferation rate (a)-(c) and increasing mean proliferation rate (d)-(f). Tumour cells divide at random rates (a) and (d). Relative proliferation (b) and (e), showing the time-varying proliferation divided by the initial proliferation. Phenotypic distributions (c) and (f) at subsequent times; insets depict the net growth ΔN in the cell number during a temporal window $[0, T]$.

53 diapause-like states have been described as a survival mechanism against chemotherapy [21,22].
 54 In this context, an initial clonal population will be subject to evolutionary pressures in a stochastic
 55 or environmental-induced way that finally shape the population structure.

56 Fluctuations in proliferation rates of clonal cancer cell populations have been observed in
 57 cultures [23–25]. The repetition of the same cell-culture experiment leads to large variations in the
 58 outcome that cannot be due only to differences in the number of cells seeded initially. This well-
 59 known fact is typically attributed to uncontrollable changes in experimental conditions. Some
 60 authors have previously accounted for these baseline variations in cell cycle duration among
 61 heterogeneous cancer cell populations [26,27] that could be indeed tightly linked to tumour
 62 response to therapy [28]. By nature, phenotypic plasticity could affect any cell trait [29], but
 63 here we will focus on proliferation as a key phenotypic characteristic in cancers. Specifically, we
 64 will study *in silico* the possibility that stochastic changes in the growth rate of clonal populations
 65 could lead to an evolutionary dynamic of that trait. Our main hypothesis would be that small
 66 phenotypic changes resulting in either faster or slower proliferation could emerge as a result
 67 of noise-induced nongenetic variability. This may lead to some variability in clonal populations
 68 that may provide the appropriate ground for selection and evolutionary dynamics. Here we
 69 will address, from a mathematical perspective, what is the outcome of those dynamics. Figure
 70 1 illustrates the underlying rationale of how fundamentally different fluctuations in proliferation
 71 eventually impact on the net growth in cell number. The upper row (a)-(c) in Fig. 1 represents
 72 the scenario in which the cellular division time randomly varies around some basal value, as
 73 we could expect from any cellular trait. In this case, cell number shows a typical exponential
 74 growth profile (1(c)) without constraints. But, what happens if we introduce stronger fluctuations
 75 in proliferation with respect to basal value accounting for phenotypic changes? One possible, and
 76 fundamentally different, scenario is depicted in the second row (d)-(f) in Fig. 1. A significantly
 77 larger cell number change ensues with respect to the preceding scenario. We elaborate below on
 78 these qualitative settings by putting forward, both discrete and continuous, mathematical models

79 with the final goal of trying to answer, or at least shed light, to the question raised earlier of what
80 is the main driving force behind the accelerated tumour growth observed in human cancers [17].

81 2 Materials and methods

82 To study the impact of phenotypic changes in proliferation on the growth dynamics of a clonal
83 tumour cell population, we resorted to two mathematical models. The first one was based on
84 a discrete simulator incorporating stochastic jumps between different proliferative states. The
85 second one, consisting of a continuous reaction-diffusion parabolic equation, recapitulated the
86 key aspects of the discrete model and allowed us to find explicit analytical formulas for the
87 temporal dynamics of the total tumour cell number, together with the mean and the standard
88 deviation in proliferation.

89 2.1 Discrete stochastic model

90 Let us first put forward a discrete stochastic model describing the growth dynamics of a clonal
91 population of tumour cells having different proliferation rates, i.e. one in which not all cells divide
92 at the same pace. To simplify the analysis, we consider a large but finite number M of allowed
93 proliferation rates ρ_i in the interval $[\rho_{\min}, \rho_{\max}]$. Each cell belongs to a proliferative state i (with
94 $i = 1, 2, \dots, M$) defined by its rate $\rho_i = (i - 1)\Delta\rho + \rho_{\min}$, where $\Delta\rho = (\rho_{\max} - \rho_{\min})/(M - 1)$. Let
95 $N_i(t)$ denote the number of tumour cells having phenotype i , thus corresponding to a rate ρ_i , at
96 time t . The total number of cells at time t is $N(t) = \sum_{i=1}^M N_i(t)$. At time $t = 0$ the population, with
97 N_0 being the initial cell number, is distributed in the phenotypic landscape around a characteristic
98 proliferation rate ρ_* having a standard deviation σ_* . To simulate the population dynamics at
99 later times, for every interval $[t, t + \Delta t]$ in steps Δt , we test whether each cell has undergone a
100 phenotypic switch, with transition rate $\Gamma_{i \rightarrow j}$, from proliferation state i to an adjacent state $j =$
101 $i \pm 1$ characterized by a proliferation rate ρ_j . No phenotypic jumps are allowed from $i = 1$ to
102 $j = 0$ and from $i = M$ to $j = M + 1$. All these switches thus give rise to a net decrease in the
103 number $N_i(t)$ of cells having the same ρ_i at time t . Similarly, phenotypic jumps with transition
104 rates $\Gamma_{j \rightarrow i}$ from adjacent proliferation states $j = i \pm 1$ into i result in a net increase in the cell
105 number $N_i(t)$. Additionally, during time interval $[t, t + \Delta t]$, mitotic and apoptotic events could
106 also take place, each either increasing or decreasing the cell number $N_i(t)$ by one unit. Combining
107 all these stochastic processes leads to a balance equation for the number of cells that, at time
108 $t + \Delta t$, have a proliferation rate ρ_i

$$\begin{aligned} N_i(t + \Delta t) = & N_i(t) - \Delta t (\Gamma_{i \rightarrow i+1} + \Gamma_{i \rightarrow i-1}) N_i(t) + \Delta t (\Gamma_{i+1 \rightarrow i} N_{i+1}(t) + \Gamma_{i-1 \rightarrow i} N_{i-1}(t)) \\ & + \Delta t \rho_i N_i(t) - \Delta t \mu N_i(t), \end{aligned} \quad (2.1)$$

109 with μ being the death rate (taken equal for all cells). In our numerical simulations using (2.1)
110 we assumed for simplicity that $\Gamma_{i \rightarrow i+1} = \Gamma_{i \rightarrow i-1} = \Gamma_{i+1 \rightarrow i} = \Gamma_{i-1 \rightarrow i} \equiv \Gamma$, hence giving rise to
111 symmetric transition jumps, except at the end points $i = 1$ and $i = M$.

112 The interplay of processes described above will result in a scenario where all phenotypic
113 changes are *inheritable*, i.e. when a cell is committed to mitosis, its progeny will be placed
114 in the same proliferative state. This gradually yields a progressive irreversibility from the
115 starting characteristic proliferation rate ρ_* towards a different phenotypic landscape. In an
116 alternative scenario, to explore the possibility of a *partial loss of inheritance* (and thus of partial
117 reversibility), we also considered the effect of adding a decay probability to the starting
118 characteristic proliferation rate ρ_* , equivalent to the time required to complete m_{cd} cell divisions.
119 Computationally, this was implemented via a transition rate $\Gamma_{i \rightarrow *}$ into a localized distribution
120 (e.g. Gaussian) centred around ρ_* for each phenotype i . In both scenarios (i.e., under *inheritance*
121 or *partial loss of inheritance*), to monitor the dynamics of the population in the phenotype space,
122 we evaluated the different population frequencies $f_i(t) = N_i(t)/N(t)$, with $i = 1, 2, \dots, M$, and
123 the mean proliferation rate $\langle \rho \rangle(t) = \sum_{i=1}^M \rho_i f_i(t)$.

2.2 Continuous reaction-diffusion-advection model

To derive a partial differential equation-based model that would help to better elucidate the time dynamics of the previous discrete stochastic framework, we considered the same processes albeit we extended the phenotypic switches assuming nonnegative transition rates $\Gamma_{i \rightarrow j}$ from a proliferation state i to another state j , where $i, j = 1, 2, \dots, M$, and phenotypic switches with transition rates $\Gamma_{j \rightarrow i}$ from proliferation states j into i . Notice that $\sum_{j=1}^M \Gamma_{i \rightarrow j} = 1$ and $\sum_{j=1}^M \Gamma_{j \rightarrow i} = 1$, although the transition rates $\Gamma_{i \rightarrow j}$ and $\Gamma_{j \rightarrow i}$ are not necessarily equal in general. The balance equation (2.1) reads now as

$$N_i(t + \Delta t) = N_i(t) - \Delta t \sum_{j=1}^M \Gamma_{i \rightarrow j} N_i(t) + \Delta t \sum_{j=1}^M \Gamma_{j \rightarrow i} N_j(t) + \Delta t \rho_i N_i(t) - \Delta t \mu N_i(t). \quad (2.2)$$

Balance equation (2.2) is quite general and encompasses the inclusion over time of new subpopulations labelled by their proliferation phenotype as their sizes become nonzero as well as the extinction of others when their cell numbers vanish. Moreover, the terms $\Gamma_{i \rightarrow j} N_i(t)$ and $\Gamma_{j \rightarrow i} N_j(t)$ can be understood as outward and inward cell currents for phenotype i , respectively.

We next perform a continuous limit approximation of (2.2). This amounts to let $\Delta t \rightarrow 0$ and $\Delta \rho \rightarrow 0$ while the transition rates $\Gamma_{i \rightarrow j} \rightarrow \infty$ and $\Gamma_{j \rightarrow i} \rightarrow \infty$. In those limits, we assume that the two quantities $D = \Delta \rho^2 / 2 \sum_{j=1}^M \Gamma_{i \rightarrow j} (j - i)^2$ and $v = \Delta \rho \sum_{j=1}^M \Gamma_{i \rightarrow j} (j - i)$ remain finite. Hence, we arrive at the following reaction-diffusion-advection equation

$$\frac{\partial n}{\partial t} = D \frac{\partial^2 n}{\partial \rho^2} - v \frac{\partial n}{\partial \rho} + \rho n - \mu n, \quad (2.3)$$

where $n = n(\rho, t)$ denotes the cell density function, such that $n(\rho, t) d\rho$ represents the number of tumour cells that, at time t , have a proliferation rate between ρ and $\rho + d\rho$. The first term on the right-hand side of (2.3) accounts for the fluctuations in the proliferation phenotype occurring with a diffusion constant D which is nonnegative. The second term describes the phenotypic drift in proliferation with a velocity v . Notice that this velocity may be positive or negative depending on the sign of $\sum_{j=1}^M \Gamma_{j \rightarrow i} (j - i)$ and is zero for fully symmetric or unbiased transitions. The third and fourth terms in (2.3) comprise the mitotic and apoptotic events. Additional mechanisms could be easily incorporated into (2.3), such as growth-limiting mechanisms preventing an unbounded increase in the total cell number. However, our main focus is to look at time scales for which the tumour has not yet achieved a large size.

The reaction-diffusion-advection equation (2.3) is further supplemented with initial and boundary conditions: $u(\rho, 0) = u_0(\rho)$ and $\frac{\partial n}{\partial \rho} = 0$, both at $\rho = \rho_{\min}$ and $\rho = \rho_{\max}$. These two zero-flux boundary conditions ensure that no cell will have a proliferation rate outside the interval $[\rho_{\min}, \rho_{\max}]$. Rather than solving (2.3), which can be carried out by means of a Green's function formalism, it is enough for our purposes to focus on time-evolving average quantities. Specifically, the total number of cells, given by $N(t) = \int_{\rho_{\min}}^{\rho_{\max}} n(\rho, t) d\rho$, the mean proliferation rate $\langle \rho \rangle(t) = \frac{1}{N(t)} \int_{\rho_{\min}}^{\rho_{\max}} \rho n(\rho, t) d\rho$, and the variance $\langle \sigma \rangle^2(t) = \frac{1}{N(t)} \int_{\rho_{\min}}^{\rho_{\max}} (\rho - \langle \rho \rangle(t))^2 n(\rho, t) d\rho$.

3 Results

3.1 Quantifying the inheritable scenario

First, we simulated the fully inheritable case in a time frame of $T = 30$ days by means of the discrete stochastic model presented in Subsection 2.1. This time frame was sufficiently short to discard relevant mutational events. An example of a typical outcome is shown in Fig. 2(a). Even when the phenotypic transitions were fully symmetric, the system spontaneously drifted towards higher proliferation values, with the mean proliferation rate $\langle \rho \rangle(t)$ reaching levels more than two times larger than the initial one ρ_* [see inset Fig. 2(a)]. Also, a broadening in the phenotype landscape was apparent as time passed. In addition, the reaction-advection-diffusion

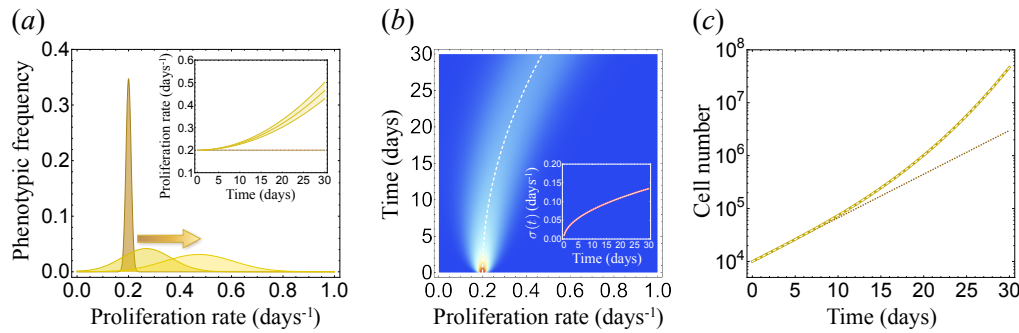


Figure 2. Computational results of the evolutionary dynamics in the landscape of the clonal tumour cell population studied in the scenario with full phenotype inheritance. (a) Phenotypic frequency at times $t = 0, 15,$ and 30 days (from left to right) of a typical run using the discrete stochastic model. The inset shows a time-dependence of the mean proliferation rate as an increasing broadening band, whereas the dotted line corresponds to a constant proliferation rate $\rho_* = 0.2$ days $^{-1}$. (b) Pseudocolor plot of the population cell density for $\rho \in [0, 1]$ days $^{-1}$ and $t \in [0, 30]$ days computed from the continuous reaction-advection-diffusion model (2.3). The dashed white line indicates the mean proliferation rate $\langle \rho \rangle(t)$ of the distribution as predicted by Eq. (3.5). The inset shows the standard deviation $\langle \sigma \rangle(t)$ from the solution of (2.3) (thick reddish curve) and the analytical formula (3.6) (overlapping dashed white curve). (c) Dynamics of the total cell population $N(t)$ from the solution of (2.3) (thick golden curve) and the analytical formula (3.4) (overlapping dashed white curve). The dotted line corresponds to the case of a purely exponential growth with a constant proliferation rate ρ_* . Numerical values used: For the discrete stochastic model $\Gamma = 6.0$ days $^{-1}$, $M = 101$ nodes, $\Delta t = 1$ h, whereas the number of simulation runs was equal to 50. For the continuous reaction-advection-diffusion model, $D = 3.0 \times 10^{-4}$ days $^{-3}$ and $v = 0$ days $^{-2}$. For both the discrete and the continuous models, we used an initial Gaussian distribution centred around $\rho_* = 0.2$ days $^{-1}$ and initial standard deviation $\sigma_* = 0.01$ days $^{-1}$. Also, $\mu = 0.01$ days $^{-1}$, $N_0 = 10^4$ tumour cells, $\rho_{\min} = 0$ day $^{-1}$ and $\rho_{\max} = 1$ day $^{-1}$.

166 model allowed us to reproduce these features in the same time frame, as depicted in Fig. 2(b),
 167 together with the standard deviation rate [inset Fig. 2(b)]. Moreover, both models predicted that
 168 the total cell population, when plotted in a logarithmic scale, increased much faster than a simple
 169 exponential growth, as shown in Fig. 2(c).

170 To determine the underlying explicit time dependences of all these distinctive characteristics,
 171 and hence gain further insight, we employed the reaction-advection-diffusion model to compute
 172 the time derivatives of $N(t)$, $\langle \rho \rangle(t)$ and $\langle \sigma \rangle^2(t)$ using (2.3). These led to the following ordinary
 173 differential equations

$$\frac{dN}{dt} = -\mu N(t) + \langle \rho \rangle(t) N(t), \quad (3.1)$$

174 for the total cell number and

$$\frac{d\langle \rho \rangle}{dt} = v + \langle \sigma \rangle^2(t), \quad (3.2)$$

175 for the mean proliferation rate. In deriving (3.1) and (3.2) we neglected the boundary values
 176 $n(\rho_{\max}, t)$ and $n(\rho_{\min}, t)$, a valid assumption when the cell population does not reach significant
 177 levels at the end points of the proliferation interval. Moreover, when $n(\rho, t)$ was assumed to have
 178 a Gaussian distribution with initial mean proliferation rate ρ_* and standard deviation σ_* , we
 179 arrived at a third ordinary differential equation

$$\frac{d\langle \sigma \rangle^2}{dt} = 2D, \quad (3.3)$$

180 for the variance.

181 The three differential equations (3.1)-(3.3) constitute an exactly solvable model. The first one
182 yields

$$N(t) = N_0 e^{-\mu t + \rho_* t + \frac{v t^2}{2} + \frac{\sigma_*^2 t^2}{2} + \frac{D t^3}{3}}, \quad (3.4)$$

183 with N_0 being the initial population. Thus, (3.4) shows that the total cell population evolves
184 in a *fundamentally different* fashion than a simple exponential growth $N(t) = N_0 e^{\rho_* t}$, the latter
185 occurring if no phenotypic changes take place in the initial proliferation rate.

186 For the mean proliferation rate we find

$$\langle \rho \rangle(t) = \rho_* + \left(v + \sigma_*^2 \right) t + D t^2. \quad (3.5)$$

187 Equation (3.5) accounts for the drift in the mean proliferation seen in all of our simulations, which
188 is quadratic with time. Notice that even in the absence of the drift velocity ($v = 0$), $\langle \rho \rangle(t)$ still
189 increases with time, the dominant contribution being due to the stochastic fluctuations embodied
190 in the diffusion coefficient D and, to a lesser extent, to the initial variability σ_* .

191 The time dependence of the standard deviation is

$$\langle \sigma \rangle(t) = \sqrt{\sigma_*^2 + 2Dt}, \quad (3.6)$$

192 which provides another explicit and simple expression for the broadening in the phenotype
193 landscape observed in our numerical simulations. This form for the standard deviation is
194 characteristic of other standard diffusive processes [30].

195 Figures 2(b) and 2(c) also compare the numerical solutions of the mean proliferation rate,
196 the standard deviation and the cell number obtained from (2.3) and formulas (3.4)-(3.6) giving
197 additional confirmation of the internal consistency of our findings. Hence, in the scenario where
198 full phenotype inheritance occurs, three distinctive features arise: a broadening in the phenotype
199 landscape, a drift in the mean proliferation and a total cell population growing faster than a classic
200 exponential law.

201 3.2 Quantifying the partially inheritable scenario

202 We then considered the scenario of a partial loss of inheritance in the phenotypic traits by
203 assuming that all phenotypes have a probability $\Gamma_{i \rightarrow *}$ to revert to the basal phenotype with
204 proliferation rate ρ_* . As in the inheritable scenario, a drift of the mean proliferation rate $\langle \rho \rangle(t)$
205 towards higher values with time was observed [see Fig. 3(e)], although the magnitude of this
206 drift was smaller as the relative importance of $\Gamma_{i \rightarrow *}$ increased. Another visible difference from
207 Fig. 2 with the full phenotype inheritance scenario is that the distribution displays a bimodal
208 profile for a certain range of $\Gamma_{i \rightarrow *}$, evidencing the coexistence of a peak corresponding to the
209 clonal population distributed around the initial proliferation rate ρ_* and a second broader peak
210 comprising the more *evolved* phenotypes [see Fig. 3(a-d)]. The standard deviation of the $\langle \sigma \rangle(t)$
211 phenotypic distribution increases in time for all values for the *reverse transition rate*. Reasonably,
212 this increase is less impressive as the reverse transition rate grows, but the increase in phenotypic
213 variability is robust across all tested conditions (Fig. 3(f)). Also, faster than a simple exponential
214 growth occurred in the population [Fig. 3(g)] the magnitude of which was modulated by the
215 partial phenotypic inheritance condition embodied in $\Gamma_{i \rightarrow *}$.

216 4 Discussion

217 In this study we put forward a mathematical model based on stochastic phenotypic transitions.
218 For simplicity, and since we were mainly interested in characterising how and why tumour
219 growth accelerates in time, we focused on proliferation. It is already known that tumour cells have
220 a higher growth rate than proliferative non-tumoral tissues. Clonal cell lines exhibit also a higher
221 frequency of random monoallelic expression that could increase phenotypic plasticity and spread
222 the probability of success in a changing environment without altering the population identity.

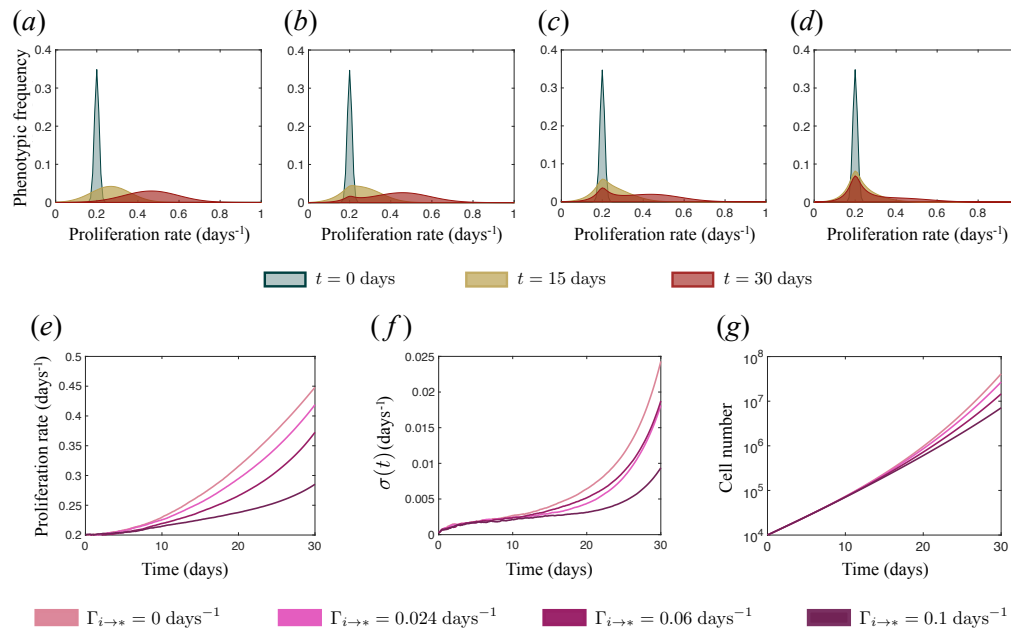


Figure 3. Computational results of the evolutionary dynamics in the landscape of the clonal tumour cell population studied in the scenario of partial loss of inheritance. (a)-(d) Phenotypic frequency at times $t = 0, 15,$ and 30 days for different values of the transition rate $\Gamma_{i \rightarrow *}$: (a) $\Gamma_{i \rightarrow *} = 0 \text{ days}^{-1}$, (b) $\Gamma_{i \rightarrow *} = 0.024 \text{ days}^{-1}$, (c) $\Gamma_{i \rightarrow *} = 0.06 \text{ days}^{-1}$, (d) $\Gamma_{i \rightarrow *} = 0.12 \text{ days}^{-1}$. (e) Time-dependence of the mean proliferation corresponding to the cases (a)-(d). (f) Time-dependence of the standard deviation corresponding to the cases (a)-(d). (g) Dynamics of the total cell population corresponding to the cases (a)-(d).

223 In this study our initial setting consisted of a genetically homogeneous clonal population, with
 224 all cells having a growth rate concentrated around a certain value. These cells were allowed to
 225 slightly increase or decrease their growth rate in time with equal probability and thus explore
 226 a landscape of proliferation states while keeping a hypothetical common genotype. One key
 227 prediction of the mathematical models developed in this work was that the sole action of
 228 stochastic phenotypic transitions, leads to a growth of the total clonal tumour cell population
 229 that is fundamentally much faster than classical exponential growth. Besides the recent findings
 230 of explosive tumour growth in several types of cancers [17], it is also intriguing to look at other
 231 natural contexts where dramatic increases in other population species may also take place, such as
 232 cyanobacteria and algae blooms occurring in eutrophic waters [31], revealing the need for further
 233 explorations within the interplay between oncology and ecology via evolutionary theory.

234 Phenotypic plasticity together with noisy gene and protein levels expression has been pointed
 235 out by means of next-generation sequencing techniques such as single cell RNA-sequencing or
 236 tissue-specific differentially methylated regions (tDMRs), giving an increasing importance to the
 237 distribution of gene expression levels or epigenetics marks beyond the classical genocentric point
 238 of view [32]. This stochastic phenomenon has also been reported at many other levels in nature,
 239 including differing levels of resistance to antibiotics in genetically identical bacteria or even the
 240 stochastic mechanism underlying the development of trichromatic vision of human individual
 241 cone cells [33].

242 Many authors have previously analysed evolutionary cancer dynamics in phenotype-
 243 structured populations [34]. However they usually include selection pressures as a key issue to
 244 observe the consequences of this phenotypic variability. A very interesting approach to these
 245 questions from a statistical mechanics perspective suggests that the number of available states
 246 shapes tumour growth [35]. However, to the best of our knowledge, the effect of the existence of a

247 proliferation phenotypic landscape and its potential role as an underlying force having a *steering*
248 effect on the natural history of tumours has not been addressed in detail.

249 While genomic instability and driver gene mutations play an essential role in the evolutionary
250 dynamics of human cancers, the sustained increase in proliferation observed in [17], which our
251 mathematical models also predict, has some resemblance with classic Darwinian selection ideas
252 which are tightly linked to the selection of the fittest genotype (in our case phenotype). On the
253 other hand, the process found is not of a Lamarckian-type since we did not consider phenotypic
254 switches to be environmentally-driven in our models [7,36].

255 One of the novel aspects of this work is the spontaneous increase in average growth rate
256 with time. A reduction in cell cycle duration over time had previously been described under
257 therapy-induced cell death [28]. There it was assumed that the tumour population consisted
258 of cells with different albeit intrinsic and fixed proliferation rates. These were inherited and
259 microenvironmental-independent without undergoing any changes in the simulations. In our
260 models phenotypic diversity emerges from a clonal population that continuously experiences
261 stochastic transitions which may be small but eventually drive the tumour cells towards more
262 proliferative phenotypes. This diffusion in phenotype landscape reminds us of spread dynamics
263 of invasive species, in which the rate of new site colonization is not constant over time as has been
264 proved in a variety of biological kingdoms, from virus to vertebrates [37].

265 Adaptive plasticity could be considered as a trait itself and consequently be subject to
266 evolutionary processes. However, we could expect that it does not play such an important role
267 in a 'constant', non-tumour, environment. Cancer cells are exposed to changing environmental
268 conditions across tumour life history and this may lead to a short-term evolutionary response
269 where genetic variation would not be the main driving force. Phenotypic diversity is a convenient
270 strategy for the success of population expansions in a broad range of contexts. Although it is
271 challenging to test this kind of hypothesis at the laboratory due to the required long time-scale
272 (as a consequence of long individual lifespan), some attempts in unicellular organisms have been
273 reported in the literature. Those evidences reflect that at short time scales, phenotypic variations
274 are key as a strategy to succeed in fluctuating environments as shown in *Chlamydomonas* [38] and
275 *Lactobacillus sp.* [39], also allowing for specialization in the long-term, as shown by *Escherichia coli*
276 culture over 2000 generations under an alternating temperature regimen [40]. The behaviour of
277 subclonal populations interacting within the constraints of the tumour microenvironment could
278 resemble the dynamics of the interaction of functional groups of species with variation in resource
279 exploitation ability and environmental requirements. Although phenotypic diversity implies an
280 additional productivity cost for the functional group, a higher phenotypic variance seems to
281 increase the long run performance [16].

282 Another interesting point concerns the role of inheritance of phenotypic modifications. It
283 is already known that phenotypic modifications in somatic cells can be passed on from one
284 generation to another by mitosis as stated previously in the fully inheritable scenario [42,43]
285 and they do not necessarily reverse after the inducing agent ceases [44]. In fact, increasing
286 evidence suggest that adaptation can be graded. Short-term stress would evoke tiny modifications
287 in gene expression through signalling-mediated regulation of gene expression. On the other
288 hand, a sustained stress situation could lead to a more radical switch in cell state, through
289 epigenetic regulation or positive feedback loops, and hence drive to a permanent phenotypic
290 modification [45–47]. We considered important to reflect those different inheritance patterns
291 in our work through the partially inheritable scenario. Our results indicate that the shift
292 towards a more aggressive average profile in the tumour phenotypic distribution is qualitatively
293 robust across both scenarios, even when modifying the reverse transition rate. The relationship
294 between this shift in proliferation phenotypic distribution and spatial heterogeneity remains
295 to be explored. Microenvironmental spatial heterogeneity due, for example, to the gradients
296 of nutrients and metabolic waste generated by tumour cells [48] might also affect that reverse
297 transition rate. The availability of physical space and new niches for dispersal and colonization
298 might also accelerate the shift in the tumour average proliferation rate [49–51]. Indeed, the

299 theoretical location of evolution at the tumour boundary has been previously reported [52]
300 and the highest proliferation activity seems to be located also at the tumour edge, specially in
301 poor prognosis cases, as it was recently underlined in two cohorts of breast and lung cancer
302 patients [53].

303 The broadening in the phenotype landscape predicted by our models may play a key role
304 not only in the heterogeneity of the clonal tumour cell population, but also in the emergence
305 of resistance mechanisms under the administration of cytotoxic therapies [7]. Although these
306 may successfully target the most proliferative cells, eventually those in the lower spectrum
307 of the phenotype landscape would be able to repopulate the fastest proliferation cell states.
308 Phenotypic diversity is a convenient strategy for the success of population expansions in a broad
309 range of contexts. A better understanding of the fundamental biological processes underlying
310 phenotypical plasticity as a source of intratumoral heterogeneity might be useful for tumour
311 containment or implementing adaptive therapies [13,54], and, ultimately, for better design of
312 therapeutic strategies.

313 In conclusion, in the context of mathematical models displaying phenotype plasticity, we
314 have observed three distinctive features: a broadening in the phenotype landscape, a drift in
315 the mean proliferation and a total cell population growing faster than classic exponential laws.
316 Our models were conceptually simple and can be extended along many directions, including
317 not only spatial effects (e.g. saturation), other traits besides proliferation, as well as more
318 cell subpopulations (e.g. immune cells). The main predictions seem to be robust enough for
319 experimental validation. It is remarkable that these effects emerge spontaneously in the absence of
320 selection pressures and are independent of initial seeding and phenotypic switching probability.
321 When phenotypic traits were allowed to be lost partially, resembling the dilution of epigenetic
322 marks as cell division progresses, the effects were still preserved. This evolution towards a more
323 aggressive phenotype would undoubtedly be accentuated by the presence of selection pressures
324 in the tumour microenvironment. Furthermore, we cannot ignore that this stochastic variation
325 is probably affecting almost any cell trait and consequently tumour cell interactions with other
326 tumour cells and also with the surrounding tissue. However, our results indicate that the existence
327 of this stochastic non-genetic variability in the proliferation rate seems enough to spontaneously
328 drive to a more aggressive tumour average phenotype.

329 **Data Accessibility.** Simulations were conducted in MATLAB (version R2020a). Code files for the
330 discrete model simulations are publicly accessible at: [https://github.com/molabEvoDynamics/rep_](https://github.com/molabEvoDynamics/rep_StochasticFluctuationsDriveNonGeneticEvolution)
331 [StochasticFluctuationsDriveNonGeneticEvolution](https://github.com/molabEvoDynamics/rep_StochasticFluctuationsDriveNonGeneticEvolution). [55]

332 **Authors' Contributions.** G.F.C. and V.M.P.-G. formulated the hypothesis and designed the research. C.O.-
333 S., G.F.C. and V.M.P.-G. performed the research. C.O.-S., G.F.C. and V.M.P.-G. wrote the paper. All authors
334 gave final approval for publication.

335 **Competing Interests.** The authors report no conflicts of interest.

336 **Funding.** This research has been supported by the James S. Mc. Donnell Foundation (USA) 21st Century
337 Science Initiative in Mathematical and Complex Systems Approaches for Brain Cancer (Collaborative award
338 220020450), the Spanish Ministerio de Ciencia e Innovación (grant number PID2019-110895RB-I00), Junta de
339 Comunidades de Castilla-La Mancha (grant nos. SBPLY/17/180501/000154 and SBPLY/19/180501/000211).
340 C.O.-S. received support from Asociación Española Contra el Cáncer (grant number 2019-PRED-28372).

341 **Acknowledgements.** We thank Juan Jiménez-Sánchez and Jesús Bosque-Martínez for the fruitful scientific
342 discussions and Juan Antonio Delgado for his very useful contributions in ecology and evolutionary theory
343 contextualization.

344 References

- 345 1. Laland KN, Uller T, Feldman MW, Sterelny K, Müller GB, Moczek A, Jablonka E, Odling-Smee
346 J. 2015 The extended evolutionary synthesis: its structure, assumptions and predictions. *Proc.*

- 347 *R. Soc. Lond. B* **282** 20151019. (doi:10.1098/rspb.2015.1019)
- 348 2. Nowell PC. 1976 The clonal evolution of tumor cell populations. *Science* **194**, 23–28.
- 349 (doi:10.1126/science.959840)
- 350 3. Cairns J. 1975. Mutation selection and the natural history of cancer. *Nature* **255**, 197–200.
- 351 (doi:10.1038/255197a0)
- 352 4. Lipinski KA, Barber LJ, Davies MN, Ashenden M, Sottoriva A, Gerlinger M. 2016 Cancer
- 353 evolution and the limits of predictability in precision cancer medicine. *Trends Cancer* **2**, 49–63.
- 354 (doi:10.1016/j.trecan.2015.11.003)
- 355 5. Greaves M. 2015 Evolutionary determinants of cancer. *Cancer Discov.* **5**, 806–821.
- 356 (doi:10.1158/2159-8290.CD-15-0439)
- 357 6. Dagogo-Jack I, Shaw AT. 2017 Tumour heterogeneity and resistance to cancer therapies. *Nat.*
- 358 *Rev. Clin. Oncol.* **15**, 81–94. (doi:10.1038/nrclinonc.2017.166)
- 359 7. Álvarez-Arenas A, Podolski-Renic A, Belmonte-Beitia J, Pesic M, Calvo GF. 2019 Interplay of
- 360 Darwinian selection, Lamarckian Induction and microvesicle transfer on drug resistance in
- 361 cancer. *Sci. Rep.* **9**, 9332. (doi:10.1038/s41598-019-45863-z)
- 362 8. Marine JC, Dawson SJ, Dawson MA. 2020 Non-genetic mechanisms of therapeutic resistance
- 363 in cancer. *Nat. Rev. Cancer* **20**, 743–756. (doi:10.1038/s41568-020-00302-4)
- 364 9. McGranahan N, Swanton C. 2017 Clonal heterogeneity and tumor evolution: past, present,
- 365 and the future. *Cell* **168**, 613–628. (doi:10.1016/j.cell.2017.01.018)
- 366 10. Goldberg AD, Allis CD, Bernstein E. 2007 Epigenetics: a landscape takes shape. *Cell* **128**, 635–
- 367 638. (doi:10.1016/j.cell.2007.02.006)
- 368 11. Huang S. 2021 Reconciling non-genetic plasticity with somatic evolution in cancer. *Trends*
- 369 *Cancer* **7**, 309–322. (doi:10.1016/j.trecan.2020.12.007)
- 370 12. Butler G, Keeton SJ, Johnson LJ, Dash PR. 2020 A phenotypic switch in the dispersal strategy
- 371 of breast cancer cells selected for metastatic colonization. *Proc. R. Soc. B* **287**, 20202523.
- 372 (doi:10.1098/rspb.2020.2523)
- 373 13. Gupta PB, Pastushenko I, Skibinski A, Blanpain C, Kuperwasser C. 2019 Phenotypic plasticity:
- 374 driver of cancer initiation, progression, and therapy resistance. *Cell Stem Cell* **24**, 65–78.
- 375 (doi:10.1016/j.stem.2018.11.011)
- 376 14. Chiou SH, et al. 2008 Positive correlations of Oct-4 and Nanog in oral cancer stem-
- 377 like cells and high-grade oral squamous cell carcinoma. *Clin. Cancer Res.* **14**, 4085–4095.
- 378 (doi:10.1158/1078-0432.CCR-07-4404)
- 379 15. Gupta PB, Fillmore CM, Jiang G, Shapira SD, Tao K, Kuperwasser C, Lander ES. 2011
- 380 Stochastic state transitions give rise to phenotypic equilibrium in populations of cancer cells.
- 381 *Cell* **146**, 633–644. (doi:10.1016/j.cell.2011.07.026)
- 382 16. Norberg J, Swaney DP, Dushoff J, Lin J, Casagrandi R. 2001 Phenotypic diversity and
- 383 ecosystem functioning in changing environments: a theoretical framework. *Proc. Natl. Acad.*
- 384 *Sci. USA* **98**, 11376–11381. (doi:10.1073/pnas.171315998)
- 385 17. Pérez-García VM et al. 2020 Universal scaling laws rule explosive growth in human cancers.
- 386 *Nat. Phys.* **16**, 1232–1237. (doi:10.1038/s41567-020-0978-6)
- 387 18. Vogelstein B, Papadopoulos N, Velculescu VE, Zhou S, Diaz LA, Kinzler KW. 2013 Cancer
- 388 genome landscapes. *Science* **340**, 1546–1558. (doi:10.1126/science.1235122)
- 389 19. Huang S. 2013 Genetic and non-genetic instability in tumor progression: link between the
- 390 fitness landscape and the epigenetic landscape of cancer cells. *Cancer Metastasis Rev.* **32**, 423–
- 391 448. (doi:10.1007/s10555-013-9435-7)
- 392 20. Battle E, Clevers H. 2017 Cancer stem cells revisited. *Nat. Med.* **23**, 1124–1134.
- 393 (doi:10.1038/nm.4409)
- 394 21. Easwaran H, Tsai HC, Baylin SB. 2014 Cancer epigenetics: tumor heterogeneity, plasticity of
- 395 stem-like states and drug resistance. *Mol. Cell* **54**, 716–727. (doi:10.1016/j.molcel.2014.05.015)
- 396 22. Rehman SK et al. 2021 Colorectal cancer cells enter a diapause-like DTP state to survive
- 397 chemotherapy. *Cell* **184**, 226–242. (doi:10.1016/j.cell.2020.11.018)
- 398 23. Buehring GC, Williams RR. 1976 Growth rate of normal and abnormal human mammary
- 399 epithelia in cell culture. *Cancer Res.* **36**, 3742–3747.

- 400 24. Smith HS, Lan S, Ceriani R, Hackett AJ, Stamper MR. 1981 Clonal proliferation of cultured
401 nonmalignant and malignant human-breast epithelia. *Cancer Res.* **41**, 4637–4643.
- 402 25. Frick P, Paudel B, Tyson D, Quaranta V. 2015 Quantifying heterogeneity and
403 dynamics of clonal fitness in response to perturbation. *J. Cell Physiol.* **230**, 1403–1412.
404 (doi:10.1002/jcp.24888)
- 405 26. Greene JM, Levy D, Herrada SP, Gottesman MM, Lavi O. 2016 Mathematical modeling reveals
406 that changes to local cell density dynamically modulate baseline variations in cell growth and
407 drug response. *Cancer Res.* **76**, 2882–2890. (doi: 10.1158/0008-5472.CAN-15-3232)
- 408 27. Powathil GG, Gordon KE, Hill LA, Chaplain MA. 2012 Modelling the effects of cell-
409 cycle heterogeneity on the response of a solid tumour to chemotherapy: biological
410 insights from a hybrid multiscale cellular automaton model. *J. Theor. Biol.* **308**, 1–19. (doi:
411 10.1016/j.jtbi.2012.05.015)
- 412 28. Tzamali E, Tzedakis G, Sakkalis V. 2020 Modeling how heterogeneity in cell cycle length
413 affects cancer cell growth dynamics in response to treatment. *Front. Oncol.* **10**, 1552.
414 (doi:10.3389/fonc.2020.01552)
- 415 29. Hanahan D, Weinberg RA. 2011 Hallmarks of cancer: the next generation. *Cell* **144**, 646–674.
416 (doi:10.1016/j.cell.2011.02.013)
- 417 30. Codling EA, Plank MJ, Benhamou S. 2008 Random walk models in biology. *J. R. Soc. Interface*
418 **5**, 813–834 (doi:10.1098/rsif.2008.0014)
- 419 31. Davis TW, Berry DL, Boyer GL, Gobler CH. 2009 The effects of temperature and nutrients on
420 the growth and dynamics of toxic and non-toxic strains of *Microcystis* during cyanobacteria
421 blooms. *Harmful Algae* **8** 715–725. (doi:10.1016/j.hal.2009.02.004)
- 422 32. Soltani M, Vargas-Garcia CA, Antunes D, Singh A. 2016 Intercellular Variability in Protein
423 Levels from Stochastic Expression and Noisy Cell Cycle Processes. *PLoS Comput. Biol.* **12**,
424 e1004972. (doi:10.1371/journal.pcbi.1004972)
- 425 33. Geiler-Samerotte KA, Bauer CR, Li S, Ziv N, Gresham D, Siegal ML. 2013 The details in the
426 distributions: why and how to study phenotypic variability. *Curr. Opin. Biotechnol.* **24**:752–759.
427 (doi:10.1016/j.copbio.2013.03.010)
- 428 34. Ardaševa A, Anderson ARA, Gatenby RA, Byrne HM, Maini PK, Lorenzi T. 2020 A
429 comparative study between discrete and continuum models for the evolution of competing
430 phenotype-structured cell populations in dynamical environments, *Phys. Rev. E* **102**, 042404.
431 (doi:10.1103/PhysRevE.102.042404)
- 432 35. West J, Newton PK. 2019 Cellular interactions constrain tumor growth. *Proc. Natl. Acad. Sci.*
433 *USA* **116**, 1918–1923. (doi:10.1073/pnas.1804150116)
- 434 36. Feinberg AP, Irizarry R A. 2010 Stochastic epigenetic variation as a driving force of
435 development, evolutionary adaptation, and disease. *Proc. Natl. Acad. Sci. USA* **107**, 1757–1764.
436 (doi:10.1073/pnas.0906183107)
- 437 37. Arim M, Abades SR, Neill PE, Lima M, Marquet PA. 2006 Spread dynamics of invasive species.
438 *Proc. Natl. Acad. Sci. USA* **103**, 374–378. (doi:10.1073/pnas.0504272102)
- 439 38. Reboud X, Bell G. 1997 Experimental evolution in *Chlamydomonas*. III. Evolution of specialist
440 and generalist types in environments that vary in space and time. *Heredity* **78**, 507–514.
441 (doi:10.1038/hdy.1997.79)
- 442 39. Siezen RJ, Tzeneva VA, Castioni A, Wels M, Phan HT, Rademaker JL, Starrenburg MJ,
443 Kleerebezem M, Molenaar D, van Hylckama Vlieg JE. 2010 Phenotypic and genomic diversity
444 of *Lactobacillus plantarum* strains isolated from various environmental niches. *Environ.*
445 *Microbiol.* **12** 758–73. (doi:10.1111/j.1462-2920.2009.02119.x)
- 446 40. Leroi AM, Lenski RE, Bennett AF. 1994 Evolutionary adaptation to temperature. III.
447 Adaptation of *Escherichia coli* to a temporally varying environment. *Evolution* **48** 1222–1229.
448 (doi:10.1111/j.1558-5646.1994.tb05307.x)
- 449 41. Nunney L. 2018 Size matters: height, cell number, and a person’s risk of cancer. *Proc. R. Soc. B*
450 **285**, 20181743. (doi: 10.1098/rspb.2018.1743)
- 451 42. Weinhold B. 2006. Epigenetics: the science of change. *Environ. Health Perspect.*, **114**(3), A160-
452 A167. (doi: 10.1289/ehp.114-a160).

- 453 43. Baylin SB, Jones PA. 2016. Epigenetic Determinants of Cancer. *Cold Spring Harbor perspectives*
454 *in biology*, 8(9), a019505. doi: 10.1101/cshperspect.a019505)
- 455 44. Turner BM. 2009. Epigenetic responses to environmental change and their evolutionary
456 implications. *Philos Trans R Soc Lond B Biol Sci.*, 364(1534), 3403-3418. (doi:
457 10.1098/rstb.2009.0125)
- 458 45. Brandman O, Meyer T. 2008. Feedback loops shape cellular signals in space and time. *Science*.
459 322(5900):390-5. (doi: 10.1126/science.1160617)
- 460 46. Flavahan WA, Gaskell E, Bernstein BE. 2017. Epigenetic plasticity and the hallmarks of cancer.
461 *Science*. 357(6348):eaal2380. (doi: 10.1126/science.aal2380)
- 462 47. Rambow F, Marine JC, Goding CR. 2019. Melanoma plasticity and phenotypic
463 diversity: therapeutic barriers and opportunities. *Genes Dev.* 33.(19-20), 1295-1318.
464 <https://doi.org/10.1101/gad.329771.119>
- 465 48. Carmona-Fontaine C et al. 2017. Metabolic origins of spatial organization in the
466 tumor microenvironment. *Proc. Natl. Acad. Sci. USA* 114, (11), 2934-2939. (doi:
467 10.1073/pnas.1700600114)
- 468 49. Hallatschek O, Fisher DS. 2014 Acceleration of evolutionary spread by long-range dispersal.
469 *Proc. Natl. Acad. Sci. USA* 111, E4911-4919. (doi:10.1073/pnas.1404663111)
- 470 50. Komarova NL. 2014 Spatial interactions and cooperation can change the speed
471 of evolution of complex phenotypes. *Proc. Natl. Acad. Sci. USA* 111, 10789-10795.
472 (doi:10.1073/pnas.1400828111)
- 473 51. Waclaw B et al. 2015 A spatial model predicts that dispersal and cell turnover limit
474 intratumour heterogeneity, *Nature* 525, 261-264. (doi:10.1038/nature14971)
- 475 52. Deforet M, Carmona-Fontaine C, Korolev KS, Xavier JB. 2019 Evolution at the edge of
476 expanding populations. *Am. Nat.* 194, 291-305. (doi:10.1086/704594)
- 477 53. Jiménez-Sánchez J et al. 2021 Evolutionary dynamics at the tumor edge reveal
478 metabolic imaging biomarkers. *Proc. Natl. Acad. Sci. USA* 118, e2018110118.
479 (doi:10.1073/pnas.2018110118)
- 480 54. Viossat Y, Noble R. 2021 A theoretical analysis of tumour containment. *Nat. Ecol. Evol.*
481 (doi:10.1038/s41559-021-01428-w)
- 482 55. Ortega-Sabater C, Fernández-Calvo G, Pérez-García VM. 2021 Stochastic
483 fluctuations drive non-genetic evolution of proliferation in clonal cancer cell
484 populations. [Source code] [https://github.com/molabEvoDynamics/rep_](https://github.com/molabEvoDynamics/rep_StochasticFluctuationsDriveNonGeneticEvolution)
485 [StochasticFluctuationsDriveNonGeneticEvolution](https://github.com/molabEvoDynamics/rep_StochasticFluctuationsDriveNonGeneticEvolution)